Atmos. Chem. Phys., 11, 8613–8623, 2011
www.atmos-chem-phys.net/11/8613/2011/
doi:10.5194/acp-11-8613-2011

Atmospheric Chemistry and Physics

Contributions of primary and secondary biogenic VOC tototal OH reactivity during the CABINEX (Community Atmosphere-Biosphere INteractions Experiments)-09 field campaign

S. Kim, A. Guenther, T. Karl, and J. Greenberg

ACD/NESL NCAR, P.O. Box 3000, Boulder CO, 80307, USA

Received: 2 March 2011 – Published in Atmos. Chem. Phys. Discuss.: 7 March 2011
Revised: 14 July 2011 – Accepted: 29 July 2011 – Published: 24 August 2011

Abstract. We present OH reactivity measurements using the comparative reactivity method with a branch enclosure technique for four different tree species (red oak, white pine, beech and red maple) in the UMBS PROPHET tower footprint during the Community Atmosphere Biosphere INteraction EXperiment (CABINEX) field campaign in July of 2009. Proton Transfer Reaction-Mass Spectrometry (PTR-MS) was sequentially used as a detector for OH reactivity and BVOC concentrations including isoprene and monoterpenes (MT) for enclosure air. Therefore, the measurement dataset contains both measured and calculated OH reactivity from well-known BVOC. The results indicate that isoprene and MT, and in one case a sesquiterpene, can account for the measured OH reactivity. Significant discrepancy between measured OH reactivity and calculated OH reactivity from isoprene and MT is found for the red maple enclosure dataset but it can be reconciled by adding reactivity from emission of a sesquiterpene, α-farnesene, detected by GC-MS. This leads us to conclude that no significant unknown BVOC emission contributed to ambient OH reactivity from these trees at least during the study period. However, this conclusion should be followed up by more comprehensive side-by-side intercomparison between measured and calculated OH reactivity and laboratory experiments with controlled temperature and light environments to verify effects of those essential parameters towards unknown/unmeasured reactive BVOC emissions. This conclusion leads us to explore the contribution towards ambient OH reactivity (the dominant OH sink in this ecosystem) oxidation products such as hydroxyacetone, glyoxal, methylglyoxal and C4 and C5-hydroxycarbonyl using recently published isoprene oxidation mechanisms (Mainz Isoprene Mechanism II and Leuven Isoprene Mechanism). Evaluation of conventionally unmeasured first generation oxidation products of isoprene and their possible contribution to ambient missing OH reactivity indicates that the ratio of OH reactivity from unmeasured products over OH reactivity from MVK + MACR is strongly dependent on NO concentrations. The unmeasured oxidation products can contribute ~7.2 % (8.8 % from LIM and 5.6 % by MIM 2 when NO = 100 pptv) of the isoprene contribution towards total ambient OH reactivity. This amount can explain ~8.0 % (9.7 % from LIM and 6.2 % from MIM 2) of missing OH reactivity, reported by Di Carlo et al. (2004) at the same site. Further study on the contribution from further generation of unmeasured oxidation products is needed to constrain tropospheric photochemical reactivity of BVOC that have important implications for both photochemical ozone and secondary organic aerosol formation.

Correspondence to: S. Kim
(saewung@ucar.edu)

1 Introduction

Total OH reactivity is defined as the quantity of total atmospheric constituents that can react with OH. It is equivalent to the inverse of the lifetime of OH (s^{-1}) in the presence of those atmospheric constituents. The measurement results have provided quantitative information about how well reactive constituents were constrained in the atmosphere by comparing with total calculated OH reactivity from the measurement data. Lou et al. (2010) summarized the ratios of measured and calculated total OH reactivity reported in the range of 1 to 3 from 16 field campaigns. The higher ratios were often observed in rural and forested areas, where biogenic

volatile organic compounds (BVOC) are a dominant player in regional photochemistry. The unaccounted measured OH reactivity relative to calculated OH reactivity is often called "missing OH reactivity". This higher degree of missing OH reactivity in BVOC dominant regions strongly suggests significant uncertainty in constraining BVOC and their oxidation products in the atmosphere. Considering the dominance of BVOC emission relative to anthropogenic VOC emission (ten times higher; Goldstein and Galbally, 2007), this uncertainty can be a potential problem in understanding photochemical ozone and secondary organic aerosol (SOA) formation in the atmosphere, two important radiative forcing agents controlling global climate (IPCC, 2007). For this reason, a number of studies have tried to identify the sources of unexplored reactive compounds in BVOC dominated regions. The potential sources include (1) unmeasured reactive BVOC emissions, (2) unmeasured reactive oxidation products from known BVOC such as isoprene and monoterpenes (MT), and (3) uncertainties in reaction rates of BVOCs with OH that propagate to calculated OH reactivity uncertainties. Existence of unmeasured BVOC emission is supported by evidence such as: (1) temperature dependence of missing OH reactivity closely following the temperature dependence of terpenoid emission (Di Carlo et al., 2004) (2) high sesquiterpene emissions from some ecosystems that are very reactive and have not been constrained by measurements (Bouvier-Brown et al., 2009) and (3) total MT concentrations, measured by the gas-chromatography technique (GC-FID) being consistently lower than those measured by proton transfer reaction mass spectrometry (PTR-MS; Lee et al., 2005).

On the other hand, other studies have shown that (1) ambient sesquiterpene concentrations at the PROPHET site, where significant missing OH reactivity was reported, were too low to explain the descrepancy (Kim et al., 2009), (2) missing OH reactivity could be reconciled by the addition of unmeasured oxidation products estimated with a box model calculation (Lou et al., 2010), (3) new oxidation mechanisms of isoprene elucidate faster production of conventionally unmeasured oxidation products (Karl et al., 2009; Paulot et al., 2009), and (4). There is a better agreement between sensitivity-corrected PTR-MS mass spectra and speciated BVOC observations by GC for branch enclosure air than the same comparisons with ambient air inside of a ponderosa pine forest canopy (Kim et al., 2010). These studies results strongly suggest that the source of unknown reactive species in the atmosphere, in some of these locations, is poorly characterized oxidation products rather than unconstrained emitted species.

To directly explore the source of unknown reactive species, we conducted total OH reactivity measurements for four different tree species applying a branch enclosure technique in the PROPHET tower ecosystem, an isoprene dominated ecosystem, during the Community Atmosphere-Biosphere Interaction Experiment (CABINEX) field campaign in July, 2009. In this ecosystem, a significant amount of missing OH reactivity was reported by Di Carlo et al. (2004). In this study, we used the comparative reactivity method (CRM, Sinha et al., 2008) to measure total OH reactivity of emissions from individual branches using proton transfer reaction-mass spectrometry (PTR-MS). The PTR-MS system also monitored BVOC concentrations inside of the enclosure to calculate total OH reactivity from known biogenic emissions such as isoprene and MT. The comparison between the measured and the calculated total OH reactivity gives us an opportunity to quantitatively assess the contribution of missing OH reactivity from unknown BVOC emission. Although two real-time measurement systems for BVOC emissions and OH reactivity are required for ideal quantitative intercomparison considering potential quick temporal changes in BVOC emissions, we deploy one analytical system (PTR-MS) for sequential measurements. Then, we compare measured and calculated OH reactivity using a model based on variations in temperature and photosynthetically active radiation (PAR), two major physical parameters governing BVOC emission. We demonstrate that this approach will allow us to probe whether there is a systematic discrepancy between measured and calculated OH reactivity from BVOC emission that can potentially cause significant missing OH reactivity in the forest canopy air. We also present calculations using two up-to-date isoprene oxidation mechanisms (Mainz Isoprene Mechanism 2 (MIM2) Taraborrelli et al., 2009 and Leuven Isoprene Mechanism (LIM) Stavrakou et al., 2010) to assess possible contributions of unmeasured isoprene oxidation products towards total OH reactivity.

2 Methods

2.1 Branch enclosure-CRM OH reactivity measurement system

The schematic diagram of the measurement system deployed for the CABINEX field campaign is shown in Fig. 1. The CRM method for measuring total OH reactivity is thoroughly described in Sinha et al. (2008) and the potential interferences from water vapor variations are discussed in Sinha et al. (2009). We, therefore, provide a brief overview of the principle of the measurement as follows:

Step 1: a known amount of pyrrole (C_4H_4NH) is introduced into the glass reactor along with VOC-free air, which has passed through the catalytic converter. The pyrrole signal is monitored by PTR-MS.

Step 2: the UV lamp is turned on to generate OH from humidified UHP nitrogen. The pyrrole signal is expected to decrease because of rapid reaction with OH ($k_{\mathrm{OH-Pyrrole}} = 1.2 \times 10^{-10}$ cm^3 molecule^{-1} s^{-1}).

Step 3: sample air from the enclosure is introduced by switching a 3-way valve in Fig. 1. The pyrrole signal

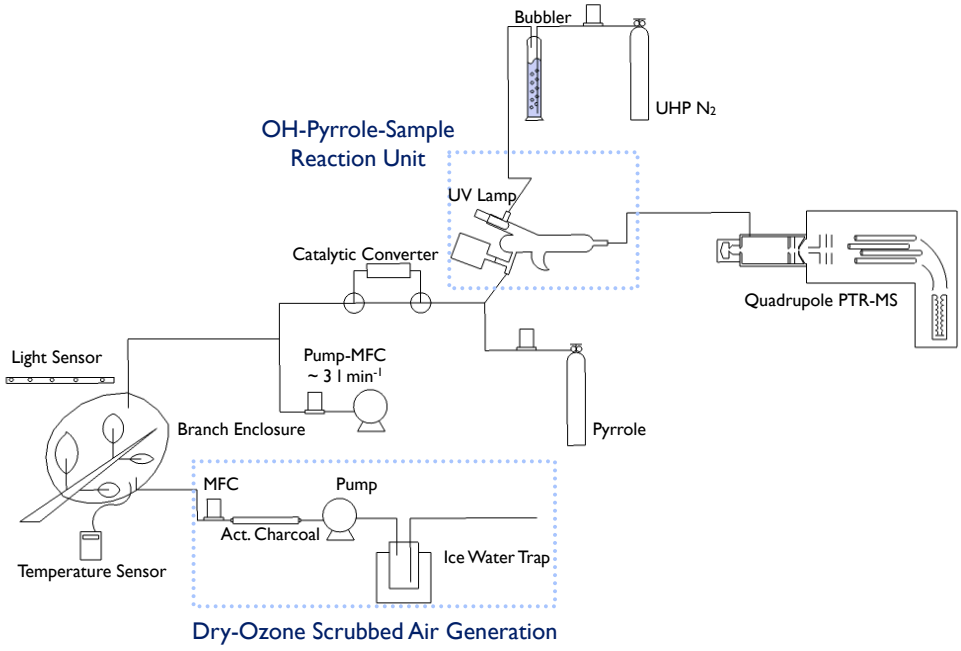

Fig. 1. A schematic diagram of the branch enclosure OH reactivity measurement system.

from Step 2 will be increased due to OH reaction competition with reactive constituents (mostly BVOC) in the sample air. Total OH reactivity of the sample air can be calculated from the signal differences as described in Sinha et al. (2008).

Step 4: the UV lamp is turned off and isoprene and MT in the sample air are analyzed with PTR-MS to assess the contribution of these compounds to the measured total OH reactivity.

In Step 2, the pyrrole concentration inside of the glass reactor was maintained at 30 ppbv, significantly higher than the concentration of OH (∼2 ppbv) to achieve the pseudo first order reaction regime so that total OH reactivity is only linearly dependent on the pyrrole concentration variation and independent of the OH concentration.

The above procedures were conducted according to a programmed routine. The volume of the Teflon branch enclosure was around 3 liters and the ozone free and VOC-scrubbed air was introduced at the rate of $\sim 6\,l\,min^{-1}$. Temperature inside of the enclosure was monitored and logged by K-type thermocouple with a portable data logger (HOBO, Onset, Pocasset, MA). Photosynthetically Active Radiation (PAR) above the enclosure was measured using a Line Quantum Sensor (LI-191, LI-COR Lincoln, NE) and the signal was also logged with a portable data logger (HOBO, Onset, Pocasset, MA). Measurements began one day after enclosing the branch in order to minimize mechanical distrubances. More specific information on the branch enclosure set-up can be found in Kim et al. (2010).

Since PTR-MS is only able to measure total MT concentration rather than speciated MT concentration, which are required to calculate the precise contribution of OH reactivity from MT, occasional sorbent cartridge (Tenax GR and Carbograph 5TD, Markes Int., Llanstrisant, UK) sampling was conducted. In addition, other terpenoids such as sesquiterpenes can be detected by the cartridge samplings. Adsorbed VOCs were measured using a Series 2 Ultra™ TD autosampler coupled to a Unity 1 thermal desorption system (MARKES International, Llantrisant, UK) interfaced with a 7890A series Gas Chromatograph/5975C Electron Impact Mass Spectrometer (GC-MS/FID) with a triple-axis detector (Agilent Technologies, Santa Clara, CA, USA). The GC was fitted with a DB5 column (0.25 mm ID × 30 m, 0.25 micron stationary phase) and was temperature programmed with an initial hold of 1 min at 35 °C and subsequent temperature rampings of $6\,°C\,min^{-1}$ to 80 °C, $3\,°C\,min^{-1}$ to 155 °C, 10 $°C\,min^{-1}$ to 190 °C, 25 $°C\,min^{-1}$ to 260 °C with a final hold of 5.2 min. to a final temperature of 300 °C.

2.2 Laboratory calibration

Before and after the field campaign, we tested the system response over a wide range of total OH reactivity. A standard gas mixture with methanol, acetonitrile, acetaldehyde, acetone, isoprene, methyl vinyl ketone, benzene, toluene, and camphene (1 ppmv ±5 %, NCAR) was mixed with zero air to generate standard samples for multipoint OH reactivity calibrations. The calibration results are summarized in Fig. 2, indicating excellent linearity over a wide range of reactivity.

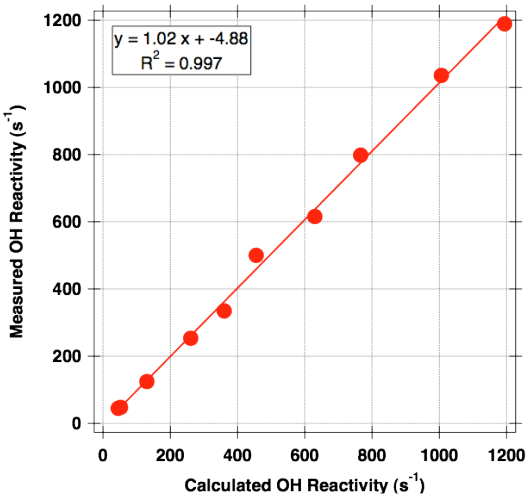

Fig. 2. Laboratory calibration results of the OH reactivity measurement system. The x-axis indicates calculated OH reactivity from standard samples and the y-axis indicates measured OH reactivity.

The limit of detection is about 15 s^{-1} for a five minute averaging time from the signals at Step 2 using Poisson statistics (3σ), which are routinely used to assess limit of detections for chemical ionization mass spectrometry techniques (Kim et al., 2009). For this study, there was no attempt to lower the detection limit because the enclosure sample was expected to have much higher OH reactivity than the assessed detection limit. Readers who are interested in ambient measurements requiring lower detection limits are referred to Sinha et al. (2010). Uncertainty of the measurement is assessed as 30 %, which includes signal fluctuation, flow fluctuation, flow controller fluctuation, uncertainty in pyrrole standard, and instrument precision.

3 Enclosure total OH reactivity measurement results and comparisons with calculated total OH reactivity from known BVOC (isoprene and monoterpenes)

Total OH reactivity measurements of enclosed branches were conducted during July of 2009. Climatologically, the experimental period was characterized by below normal temperature and above normal precipitation. Branches for enclosure measurements were selected on trees near the lab in order to reduce wall loss of potential reactive emission compounds to the sampling tubing. This constraint allowed us to sample only the understory branches.

Ortega et al. (2007) reported specific tree species composition near the PROPHET tower ecosystem and isoprene and MT basal emission rates of the five major tree species. The study reported red oak (Quercus rubra) as one of dominant isoprene emitters and white pine (Pinus strobus) as one of most dominant MT emitters in this ecosystem. The daily variations of measured and calculated total OH reactivity for the oak tree branch enclosure are presented in the bottom panel of Fig. 3 along with branch enclosure temperature and PAR variations in the upper panel. The error bar represents uncertainties of OH reactivity measurement (30 %) and calculated OH reactivity (22 %). In addition, the composition of BVOC, which was measured by sorbent cartridge sampling with GC-MS/FID analysis, from the oak tree enclosure is summarized in Table 1a. The data for the first three days were from one branch enclosure system (Oak Branch 1) and the data of July 24th was from another branch (Oak Branch 2). Except 5 July, the measured OH reactivity is within the uncertainty range of the calculated OH reactivity associated with isoprene concentrations measured by PTR-MS. For comparison purposes, in Fig. 4, afternoon temporal variations (02:00 p.m. to 06:00 p.m., local time) of measured and calculated OH reactivity are presented for 4 and 5 July along with enclosure temperature and PAR variations. The temperature and PAR variations of both days appear quite different. 4 July has a typical daily temperature pattern for cloudless conditions but the variation on 5 July indicates a few abrupt temperature changes just after the temperature reached the peak value of the day due to occasional overcasts. The differences in the measured and calculated OH reactivity can be explained by this difference. On 4 July, as temperature smoothly varies, the calculated and measured OH reactivity variations are comparable but on 5 July the temperature drops in the middle of the day causing a depressed measured OH reactivity, which was due to decreased terpenoid emissions. However, as the enclosure temperature increased while the system was operated in the BVOC measurement mode, the calculated OH reactivity indicated a big increase. Shortly after, the temperature dropped off again, while the system changed to the OH reactivity measurement mode. These differences are confirmed by PAR variations, also plotted in Fig. 4. Thus, we can understand that the significant disagreement on 5 July was actually caused by rapidly changing physical parameters that result in calculated and measured OH reactivity results that cannot be directly compared. Figure 5 illustrates daily variations of measured and calculated OH reactivity (bottom panel) and enclosure temperature and PAR above the white pine enclosure (upper panel). As summarized in Table 1a, MT are the most dominant BVOC emission of the enclosure and the calculated OH reactivity variations by MT emission are within the range of measured OH reactivity variations as shown in Fig. 5.

To quantitatively compare the measured and the calculated OH reactivity for the same conditions of PAR and temperature, the two dominant physical parameters controlling BVOC emission, one-minute averaged measured and calculated OH reactivity were plotted as a function of temperature in Fig. 6. It should be noted that the highest temperature bin data of Fig. 6b for measured OH reactivity is only based on two data points. Overall, both the measured and calculated OH reactivity datasets closely followed the exponential

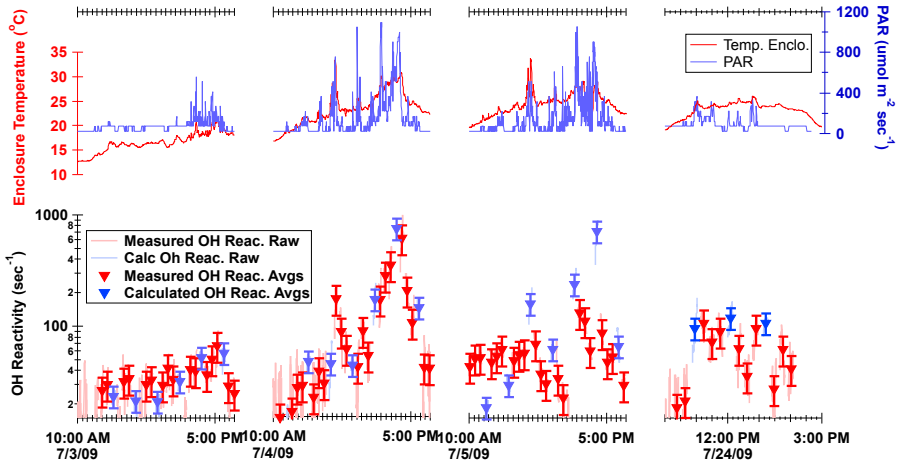

Fig. 3. (Bottom panel) Temporal variations of measured (red) and calculated (blue) OH reactivity and (top panel) temperature and PAR measurement for red oak branch enclosure (bottom panel: measured OH reactivity in the light red lines, calculated OH reactivity in the light blue lines, 20-min averaged measured OH reactivity in the red triangles, 20-min averaged calculated OH reactivity in the blue triangles).

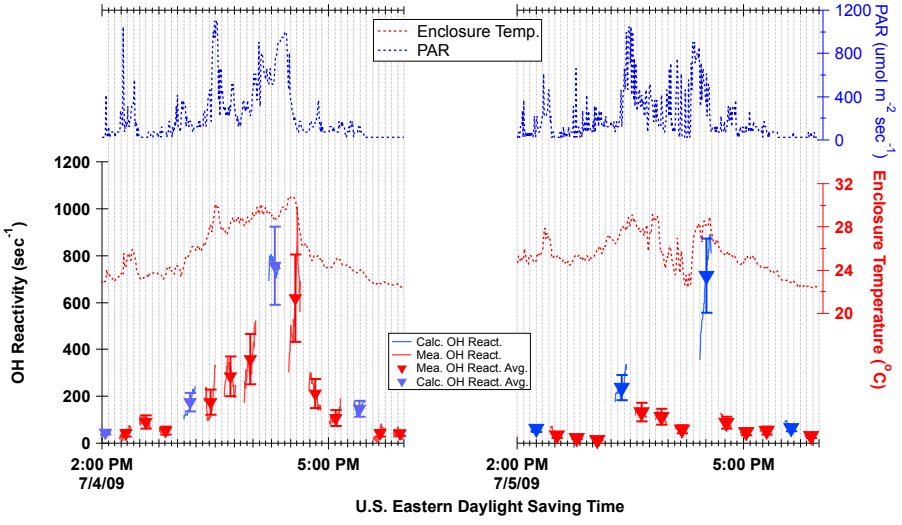

Fig. 4. A close look for variations of measured and calculated OH reactivity from the red oak enclosure, shown in Fig. 3 to examine correlations with temperature and PAR (20-min averaged measured OH reactivity in the red triangles, 20-min averaged calculated OH reactivity in the blue triangles).

function that is expected for the temperature dependence of BVOC emissions (Guenther et al., 1995). A 5 °C running averaged measured and calculated OH reactivity with color-coding of PAR on the plots clearly indicate that the difference of the measured and calculated OH reactivity in each 5 °C temperature bin can be explained by the differences in PAR. This comparison demonstrated the good agreement between measured and calculated OH reactivity. These results suggest that there is no significant missing OH reactivity associated with primary BVOC emission for red oak and white pine, which are the two main tree species dominating isoprene and MT emissions, respectively, in this ecosystem. To more quantitatively examine correlations between the physical parameters (temperature and PAR) and OH reactivity, an independently controlled environment for each parameter is required.

We also conducted model predicted OH reactivity calculation from observed temperature and PAR using BVOC emission algorithms described by Guenther et al. (2006) to compare with the measured and the calculated OH reactivity from oak and white pine branch enclosures. Figure 7a contains temporal variations of measured and calculated OH reactivity for the oak tree branch enclosure with the same notation that was used in Fig. 6. The model predicted OH reactivity is

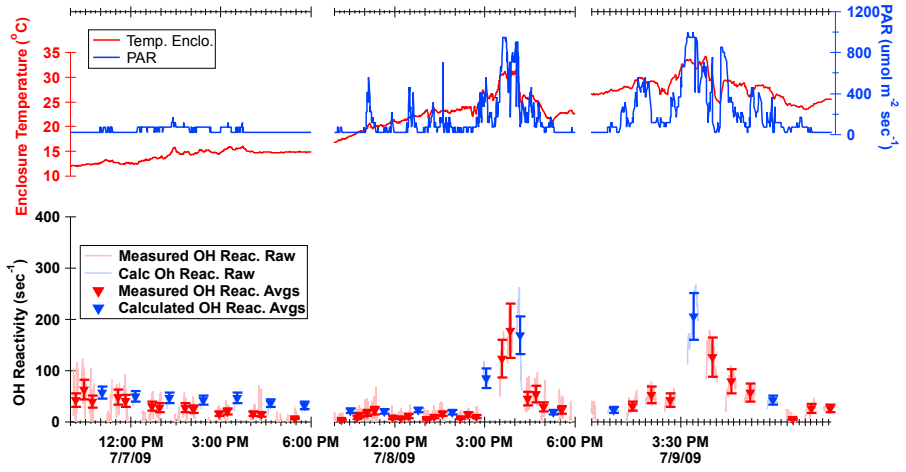

Fig. 5. (Bottom panel) Temporal variations of measured (red) and calculated (blue) OH reactivity and (top panel) temperature and PAR measurement for white pine branch enclosure (bottom panel: measured OH reactivity in the light red lines, calculated OH reactivity in the light blue lines, 20-min averaged measured OH reactivity in the red triangles, 20-min averaged calculated OH reactivity in the blue triangles).

shown as grey dotted curves. In general, the model predicted OH reactivity in 4 July agrees well with the measured and calculated OH reactivity except for two data points, showing the highest measured and calculated OH reactivity levels in the day. However, on 5 July, the model prediction shows poor correlation with the measured and calculated OH reactivity. This again may be because the model did not account for BVOC emission variations due to the rapid enclosure temperature and PAR changes during that day. Figure 7b shows the model predicted OH reactivity for the white pine branch enclosure along with the measured and calculated OH reactivity in 8 and 9 July. The model prediction agrees very well with the calculated and measured OH reactivity. This analysis again confirms that there is no significant unaccounted BVOC emission from the branch enclosures. However, it is noteworthy that when physical parameters that affect BVOC emission change rapidly, model BVOC emission predictions tend to deviate from measured values.

The upper panel of Table 1b shows the BVOC composition of a beech tree branch enclosure determined by GC-MS measurement from cartridge sampling. BVOC emission from beech in the PROPHET tower ecosystem was not previously characterized. MT were the dominant emission of the particular branch investigated and sesquiterpenes (SQT), primarily α-farnesene, composed a minor fraction of the emission. Although we measured two different beech branch enclosures during the study period, the cool and rainy weather resulted in only two days of datasets with detectable emission rates. Overall, temporal variations of the measured and calculated (only MT considered) OH reactivity show reasonable agreement as shown in Fig. 8. The cartridge sampling analysis results, in the bottom panel of Table 1b, indicate that the dominant emission from a red maple tree enclosure was α-farnesene. Since α-farnesene is a very reactive compound with OH ($k_{OH} = 3.2 \times 10^{-10}$), this results in an obvious discrepancy between measured and calculated OH reactivity with measured values that are consistently higher than calculated values when the calculated values only consider observed MT concentrations in the branch enclosure as shown in Fig. 9. The temporal variations of the calculated OH reactivity, including α-farnesene from GC-MS/FID analysis, indicated by green triangles in Fig. 8 shows much closer agreement with measured OH reactivity.

To our knowledge, this study is the first published report of direct total OH reactivity measurement using an enclosure technique to constrain missing BVOC emission. Our measurement and data analysis clearly indicate that the temporal variations of branch enclosure OH reactivity measurements of three different tree species can be explained by the variations of calculated OH reactivity from isoprene and MT, and other known BVOC. A fourth species, red maple, showed consistently higher measured OH reactivity than the levels that could not be explained by isoprene and MT but by consideration of the reactivity of a SQT, α-farnesene, we can reconcile the discrepancy between measured and calculated OH reactivity. These results, therefore, do not suggest that there is a significant unknown or unmeasured primary BVOC emission for the tree species that dominate this ecosystem.

4 Possible contributions of first generation oxidation products of isoprene to ambient total OH reactivity

If we conclude that there is no significant unknown primary BVOC emission that contributes to OH reactivity, then we must consider if there is any other source of missing OH reactivity in this forest canopy. One possibility is that unmeasured/unknown isoprene oxidation products are

Table 1. A summary of GC-MS analysis of BVOC emission speciation from (a) red oak (top panel) and white pine (bottom panel) enclosures and (b) beech (top panel) and red maple (bottom panel) enclosures.

Terpenoids	Species	Composition (%)
(a) Red Oak Enclosure BVOC Speciation		
Isoprene	isoprene	98.9
Monoterpenes	α-pinene	0.3
	β-pinene	0.3
	camphene	0.1
	β-phellandrene	0.2
	limonene	0.2
White Pine Enclosure BVOC Speciation		
Monoterpenes	α-pinene	11.7
	β-pinene	22.0
	camphene	6.9
	limonene	15.3
	3-carene	5.0
Oxygenated monotperpenes	linalool	37.1
Sesquiterpenes	α-humulene	0.2
	β-caryophyllene	0.8
(b) Beech Enclosure BVOC Speciation		
MT	α-pinene	50.9
	β-pinene	8.5
	3-carene	2.0
	d-limonene	26.2
	α-phellandrene	4.5
	β-phellandrene	2.0
SQT	α-farnesene	5.8
Maple Enclosure BVOC Speciation		
MT	Ocimene	46.7
SQT	a-farnesene	55.3

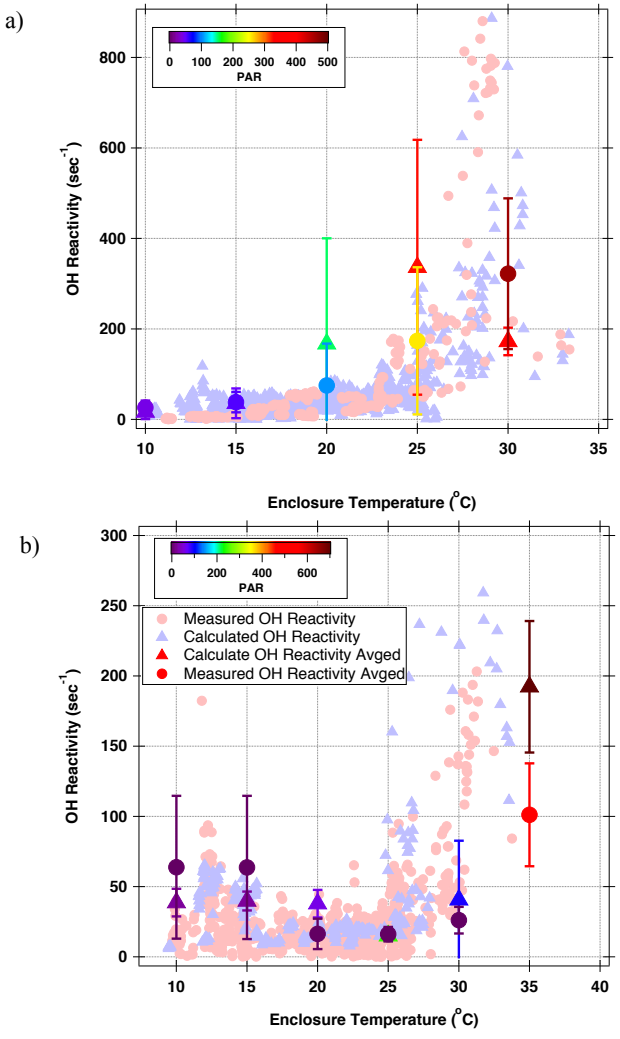

Fig. 6. Calculated (the pale blue triangles) and measured OH reactivity (the pale red circles) distribution as a function of branch enclosure temperature **(a)** red oak and **(b)** white pine branch enclosures. 5 °C running averaged calculated and measured OH reactivity is also presented with PAR color-coding. The error bars in the plots indicate 1-sigma of the statistics.

responsible since isoprene is the dominant BVOC emission in this ecosystem. Paulson and Seinfeld (1992) presented a comprehensive isoprene oxidation mechanism based on studies beginning in the late 70s and results from their chamber experiments. They confirmed that the major first oxidation products of isoprene are methyl vinyl ketone, methacrolein, formaldehyde, and alkyl nitrate under conditions of high NO_x and estimated that 22 % of the carbon was not identified. The candidates of unidentified products were speculated as "multifunctional, mostly five carbon compounds that form via allylic rearrangement". These speculated compounds were tentatively identified by PTR-MS from field experiments (Williams et al., 2001) and laboratory experiments (Zhao et al., 2004). As Paulson and Seinfeld (1992) speculated, the compounds were C4 and C5 hydroxycarbonyl compounds and their yields were estimated to be ∼31 % (Zhao et al., 2004). These findings catalyzed multi-platform (theoretical, laboratory and field) studies, revealing the complicated nature (e.g. Dibble 2004a, b, and Paulot et al., 2009) of isoprene oxidation chemistry.

Recently, Karl et al. (2009) assessed a number of isoprene oxidation chemistry mechanisms to explain unexpected high hydroxyacetone concentrations observed in the Amazon forest. Conventionally, hydroxyacetone was considered a major oxidation product of MACR by OH. The production rate of hydroxyacetone from MACR oxidation could only explain 10 % of the observed hydroxyacetone. To reconcile the discrepancy, Karl et al. (2009) proposed direct production of hydroxyacetone from isoprene oxidation by OH with a molar yield of 8.3 %. Indeed, a number of recent findings from

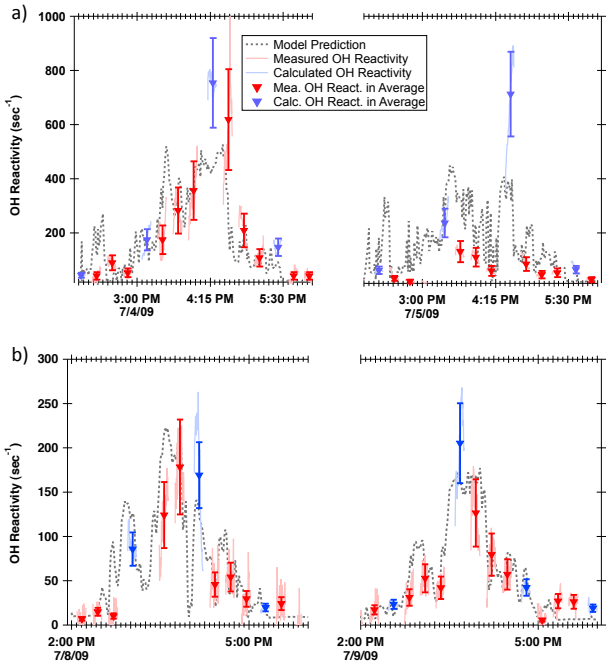

Fig. 7. The temporal variations of the emission model (see the text for details) predicted OH reactivity (in grey dotted curves) and calculated and measured OH reactivity for **(a)** the oak tree branch enclosure and **(b)** white pine tree branch enclosure.

laboratory experiments and theoretical mechanism studies report hydroxyacetone as a first generation oxidation product of isoprene. However, the reported hydroxyacetone yield from isoprene OH oxidation as the first generation product by Paulot et al. (2009) in high NO_x condition is significantly lower (3.8 %) than what Karl et al. (2009) proposed. There are several possibilities for this discrepancy. The first possibility is differences in analytical techniques. Paulot et al. (2009) used CF_3O^- ion chemistry to detect oxidation products of isoprene including hydroxyacetone. The second reason could be different NO_x conditions, critically controlling peroxy radical chemistry. This discrepancy urges more systematic laboratory studies with comprehensive measurement tools with various simulation conditions.

We evaluated possible contributions towards ambient total OH reactivity from recently published isoprene oxidation mechanisms (MIM2 and LIM), which have been embedded in global 3-D chemical transport models. Both models incorporated the new findings on isoprene oxidation chemistry and show a very strong NO dependence in their product distributions (Stavrakou et al., 2010 for LIM and Taraborelli et al., 2009 MIM2). From the oxidation product distributions estimated with the model calculation, we calculated total OH reactivity from each case and assessed the fraction from the routinely measured compounds (e.g. MVK and MACR) and the unmeasured compounds (e.g. C5, C4-hydroxycabonyl compounds, C5-hydroperoxyaldehyde (only in LIM) hydroxyacetone, glyoxal, and glycolaldehyde). Based on the isoprene daily variation observed at the PROPHET tower site in the summer of 2005 by PTR-MS, we ran a time-dependent box model to obtain isoprene first generation oxidation product production. Daily variations of OH, HO_2 and RO_2 are constrained by daily maximum concentrations of 2.5×10^6 molecules cm^{-3}, 1×10^9 molecules cm^{-3}, and 1×10^9 molecules cm^{-3}. The daily variation of OH concentration is assumed to follow daily variation of J_{NO_2} from the TUV 4.1 model run for the site. The HO_2, RO_2 daily variations are assumed to be similar to the OH daily variation and the difference from the OH variation maintained at a level of 25 % of the daytime maximum before dawn and after sunset (Tan et al., 2001).

The calculation results are presented in Fig. 10. The left panels of the figures show the diurnal variations of OH reactivity from MVK + MACR (red solid) and the unmeasured compounds (red dash) and the ratio of OH reactivity from MVK + MACR and the unmeasured compounds from the LIM oxidation scheme. Each panel shows the simulation with different NO mixing ratios as indicated in the figure. The right panels of Fig. 10 contain corresponding calculation results from the MIM2 oxidation scheme. Both schemes predict higher OH reactivity from the unmeasured compounds than OH reactivity from MVK + MACR in a low NO environment. However the ratios of OH reactivity from unmeasured compounds with MVK + MACR indicates significant differences between the mechanisms for different NO levels. Especially for 50 pptv of NO, the LIM scheme indicates that OH reactivity from unmeasured compounds is $\sim$ 3.2 times higher than that from MVK + MACR. On the other hand, the MIM2 scheme indicates $\sim$1.5 times higher OH reactivity from unmeasured compounds than OH reactivity from MVK + MACR. It is also noticeable that in the high NO simulation, MIM2 predicts higher ratios than those from LIM. These exercises suggest that the contribution of conventionally unmeasured oxygenated VOC to total OH reactivity should be carefully evaluated for appropriate NO conditions to constrain the source of missing OH reactivity in clean forest environments where relatively high missing OH reactivity has been reported. These ratios indicate that the OH reactivity contribution of first generation unmeasured oxygenated compounds could contribute to ambient total OH reactivity in the PROPET tower forest canopy. Apel et al. (2002) reported MVK, MACR, and isoprene measurement results at the PROPHET tower in 1998. The median mixing ratios of MVK, MACR, and isoprene during the daytime (10:00 a.m. to 02:00 p.m., local time) were 0.14 ppbv, 0.07 ppbv and 1.90 ppbv, respectively. Therefore, the OH reactivity ratio of MVK + MACR relative to isoprene from the ambient concentrations is 0.026. Since the PROPHET site is in the low NO_x regime (Tan et al., 2001), we applied the calculated ratios of OH reactivity from MVK + MACR and the unmeasured first generation oxidation products in low NO regime ($\sim$100 pptv of NO, S. Bertman, personal

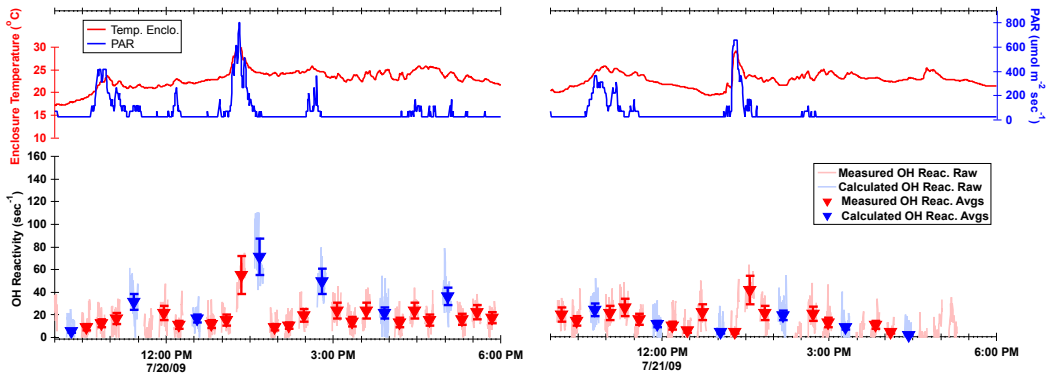

Fig. 8. (Bottom panel) Temporal variations of measured (red) and calculated (blue) OH reactivity and (top panel) temperature and PAR measurement for beech branch enclosure (bottom panel: measured OH reactivity in the light red lines, calculated OH reactivity in the light blue lines, 20-min averaged measured OH reactivity in the red triangles, 20-min averaged calculated OH reactivity in the blue triangles).

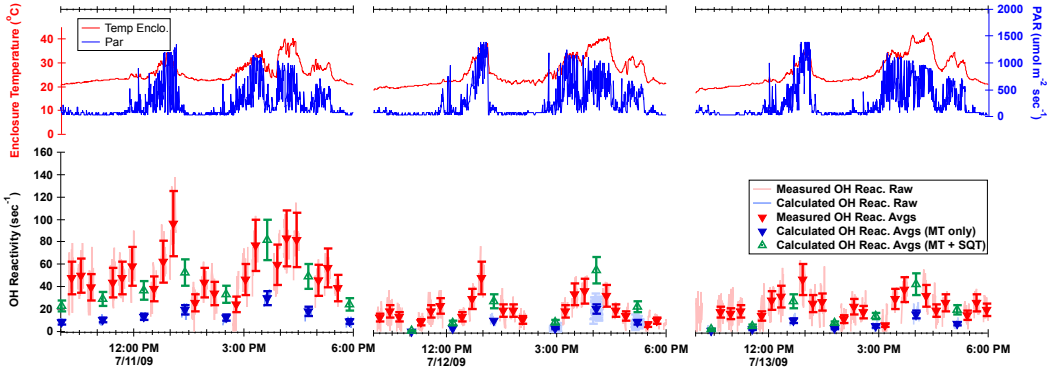

Fig. 9. (Top panel) Temporal variations of measured (red) and calculated (blue) OH reactivity and (bottom panel) temperature and PAR measurement for red maple branch enclosure. The green triangles indicate calculated OH reactivity with addition of α-farnesene emission, detected by GC-MS (see the text for detail) (bottom panel: measured OH reactivity in the light red lines, calculated OH reactivity in the light blue lines, 20-min averaged measured OH reactivity in the red triangles, 20-min averaged calculated OH reactivity in the blue triangles).

communication, 2010 and Thornberry et al., 2001) to assess potential contributions of the unmeasured first generation oxidation products of isoprene. The calculation results indicate that the unmeasured oxidation products can contribute ~7.2 % (8.8 % from LIM and 5.6 % by MIM 2) of the isoprene contribution towards total ambient OH reactivity. This amount can explain ~8.0 % (9.7 % from LIM and 6.2 % from MIM 2) of missing OH reactivity, reported by Di Carlo et al. (2004). In this analysis, we only consider the first generation isoprene oxidation products. As noted by Karl et al. (2009), the contributions from further generation oxidation products towards total OH reactivity become significant (up to 150 % of OH reactivity from isoprene) for a photochemically aged isoprene dominated air mass. Therefore, to resolve missing OH reactivity in this ecosystem our research results suggest that further investigation is needed to quantify unmeasured oxidation products of isoprene.

5 Summary and conclusion

As an activity of the CABINEX-09 field campaign, we conducted branch enclosure OH reactivity measurements on four different tree species (red oak, white pine, beech, and red maple) using PTR-MS by applying the CRM approach with a pyrrole reagent (Sinha et al., 2008). The system was set to measure OH reactivity about 75 % of the time and isoprene and MT concentrations inside of the enclosure for 25 % of the time in order to compare total OH reactivity and calculated OH reactivity from BVOC emissions with help of auxiliary measurement data such as temperature and PAR. The measurement from red oak, the main isoprene emitter in the ecosystem, and white pine, one of the main isoprene emitters, clearly indicate no significant discrepancy between measured OH reactivity and calculated OH reactivity from isoprene and MT concentrations in the branch enclosures. Branch enclosure measurements

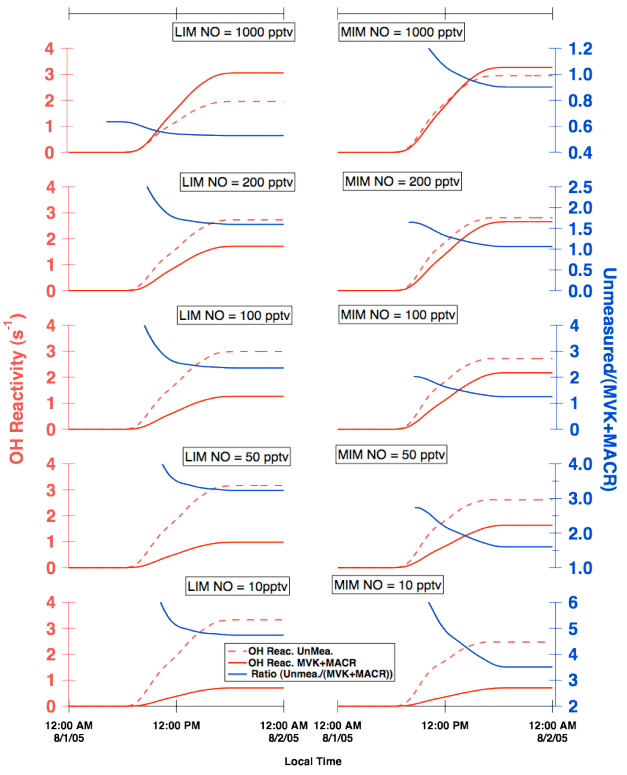

Fig. 10. Model calculated OH reactivity from MVK and MACR (the solid red line) and conventionally unmeasured isoprene first generation oxidation products explained in the text (the dashed line). The blue lines in each panel indicates the temporal variations of ratios of OH reactivity from conventionally unmeasured isoprene first generation oxidation products and OH reactivity from MVK and MACR.

of beech, which emits primarily MT, also shows reasonable agreement between measured and calculated OH reactivity. Finally, branch enclosure measurements of red maple indicated a systematic discrepancy between measured and calculated OH reactivity from only isoprene and MT. However, if we include the OH reactivity from SQT (α-farnesene), detected by GC-MS, the discrepancy could be reconciled. The results indicate that contributions of ambient OH reactivity from unaccounted/unmeasured BVOC emission should be minimal during the field experiment period although additional measurements of more tree species and individuals at the site are needed to confirm this conclusion.

To further explore the possibility that missing OH reactivity can be explained by contributions of conventionally unmeasured isoprene oxidation products such as C5, C4 hydroxycarbonyl compounds, hydroxyacetone, glyoxal, and methylglyoxal, we evaluated their contributions using two isoprene oxidation schemes (LIM and MIM2) used for regional and global tropospheric chemistry models. The evaluation results show that the conventionally unmeasured first generation products of isoprene that are produced during the day could contribute ~7.2 % of OH reactivity from ambient isoprene. This can be interpreted as accounting for ~8 % of the missing OH reactivity, reported in this ecosystem by Di Carlo et al. (2004). Karl et al. (2009) pointed out that more photochemically aged air masses have even more significant contributions of OVOC to total OH reactivity, so the contribution certainly can be even greater. These analyses suggest that we need to quantify these unconstrained isoprene oxidation products in order to resolve the source of missing OH reactivity at this forest site. As Peeters and Muller (2010) claimed from their theoretical studies, different laboratory conditions, especially NO level, can cause different distributions of oxidation products and serve as a guideline for oxidation mechanism development. This, therefore, suggests the need for more systematically NO controlled laboratory experiments along with better calibration synthesis methods. In addition, the HO_2-RO_2 ratio, which makes significant differences in oxidation product distributions (Navarro et al., 2011), should be very carefully considered in controlled laboratory experiments and interpreted for atmospheric implications (Paulot et al., 2009). This effort should be combined with the effort to characterize primary BVOC emission such as sesquiterpenes, which may contribute to total OH reactivity in some ecosystems.

Acknowledgements. We are grateful to M. A. Carroll and University of Michigan Biological Station for use of the PROPHET tower facility. We thank Tiffany Duhl for her assistance in analyzing cartridge samples. The National Center for Atmospheric Research is operated by the University Corporation for Atmospheric Research under sponsorship from the US National Science Foundation. Any opinions, findings and conclusions or recommendations expressed in this publication are those of the authors and do not necessarily reflect the views of the National Science Foundation.

Edited by: A. Hofzumahaus

References

Apel, E. C., Riemer, D. D., Hills, A., Baugh, W., Orlando, J., Faloona, I., Tan, D., Brune, W., Lamb, B., Westberg, H., Carroll, M. A., Thornberry, T., and Geron, C. D.: Measurement and interpretation of isoprene fluxes and isoprene, methacrolein, and methyl vinyl ketone mixing ratios at the PROPHET site during the 1998 intensive, J. Geophys. Res.-Atmos., 107(D3), 4034, doi:10.1029/2000JD000225, 2002.

Bouvier-Brown, N. C., Holzinger, R., Palitzsch, K., and Goldstein, A. H.: Large emissions of sesquiterpenes and methyl chavicol quantified from branch enclosure measurements, Atmos. Environ., 43, 389–401, 2009.

Di Carlo, P., Brune, W. H., Martinez, M., Harder, H., Lesher, R., Ren, X., Thornberry, T., Carroll, M. A., Young, V., Shepson, P. B., Riemer, D., Apel, E., and Campbell, C.: Missing OH reactivity in a forest: Evidence for unknown reactive biogenic VOCs, Science, 304, 722–725, 2004.

Dibble, T. S.: Intramolecular hydrogen bonding and double H-atom transfer in peroxy and alkoxy radicals from isoprene, J. Phys. Chem. A, 108, 2199–2207, doi:10.1021/JP0306702, 2004a.

Dibble, T. S.: Prompt chemistry of alkenoxy radical products of the double H-atom transfer of alkoxy radicals from isoprene, J. Phys. Chem. A, 108, 2208–2215, doi:10.1021/JP0312161, 2004b.

Goldstein, A. H. and Galbally, I. E.: Known and unexplored organic constituents in the earth's atmosphere, Environ. Sci. Technol., 41, 1515–1521, 2007.

Guenther, A., Hewitt, C. N., Erickson, D., Fall, R., Geron, C., Graedel, T., Harland, R. J., Klinger, L., Lerdau, M., Mckay, M., Pierce, T., Scholes, B., Steinbrecher, R., Tallamraju, R., Taylor, J., and Zimmerman, P.: A global model of natural volatile organic compound emission, J. Geophys. Res., 100, 8873–8892, 1995.

Guenther, A., Karl, T., Harley, P., Wiedinmyer, C., Palmer, P. I., and Geron, C.: Estimates of global terrestrial isoprene emissions using MEGAN (Model of Emissions of Gases and Aerosols from Nature), Atmos. Chem. Phys., 6, 3181–3210, doi:10.5194/acp-6-3181-2006, 2006.

IPCC: Climate change 2007-syntesis report, Geneva, Switzerland, 2007.

Karl, T., Guenther, A., Turnipseed, A., Tyndall, G., Artaxo, P., and Martin, S.: Rapid formation of isoprene photo-oxidation products observed in Amazonia, Atmos. Chem. Phys., 9, 7753–7767, doi:10.5194/acp-9-7753-2009, 2009.

Kim, S., Karl, T., Helmig, D., Daly, R., Rasmussen, R., and Guenther, A.: Measurement of atmospheric sesquiterpenes by proton transfer reaction-mass spectrometry (PTR-MS), Atmos. Meas. Tech., 2, 99–112, doi:10.5194/amt-2-99-2009, 2009.

Kim, S., Karl, T., Guenther, A., Tyndall, G., Orlando, J., Harley, P., Rasmussen, R., and Apel, E.: Emissions and ambient distributions of Biogenic Volatile Organic Compounds (BVOC) in a ponderosa pine ecosystem: interpretation of PTR-MS mass spectra, Atmos. Chem. Phys., 10, 1759–1771, doi:10.5194/acp-10-1759-2010, 2010.

Lee, A., Schade, G. W., Holzinger, R., and Goldstein, A. H.: A comparison of new measurements of total monoterpene flux with improved measurements of speciated monoterpene flux, Atmos. Chem. Phys., 5, 505–513, doi:10.5194/acp-5-505-2005, 2005.

Lou, S., Holland, F., Rohrer, F., Lu, K., Bohn, B., Brauers, T., Chang, C.C., Fuchs, H., Häseler, R., Kita, K., Kondo, Y., Li, X., Shao, M., Zeng, L., Wahner, A., Zhang, Y., Wang, W., and Hofzumahaus, A.: Atmospheric OH reactivities in the Pearl River Delta – China in summer 2006: measurement and model results, Atmos. Chem. Phys., 10, 11243–11260, doi:10.5194/acp-10-11243-2010, 2010.

Navarro, M. A., Dusanter, S., Hites, R. A., and Stevens, P. S.: Radical dependence of the yields of methacrolein and methyl vinyl ketone from OH-initiated oxidation of isoprene under NO_x-free condition, Environ. Sci. Technol., 45(3), 923–929, 2011.

Ortega, J., Helmig, D., Guenther, A., Harley, P., Pressley, S., and Vogel, C.: Flux estimates and oh reaction potential of reactive biogenic volatile organic compounds (BVOCs) from a mixed northern hardwood forest, Atmos. Environ., 41, 5479-5495, 2007.

Paulot, F., Crounse, J. D., Kjaergaard, H. G., Kroll, J. H., Seinfeld, J. H., and Wennberg, P. O.: Isoprene photooxidation: new insights into the production of acids and organic nitrates, Atmos. Chem. Phys., 9, 1479–1501, doi:10.5194/acp-9-1479-2009, 2009.

Paulson, S. E. and Seinfeld, J. H.: Development and evaluation of photooxidation mechanism for isoprene, J. Geophys. Res., 97, 20703–20715, 1992.

Peeters, J. and Muller J.-F.: HO_x radical regeneration in isoprene oxidation via peroxy radical isomerisations. II: experimental evidence and global impact, Phys. Chem. Chem. Phys., 12, 14227–14235, doi:10.1039/c0cp00811g, 2010.

Sinha, V., Williams, J., Crowley, J. N., and Lelieveld, J.: The Comparative Reactivity Method – a new tool to measure total OH Reactivity in ambient air, Atmos. Chem. Phys., 8, 2213–2227, doi:10.5194/acp-8-2213-2008, 2008.

Sinha, V., Custer, T. G., Kluepfel, T., and Williams, J.: The effect of relative humidity on the detection of pyrrole by PTR-MS for OH reactivity measurements, Int. J. Mass Spectrom., 282, 108–111, 2009.

Sinha, V., Williams, J., Lelieveld, J., Ruuskanen, T. M., Kajos, M. K., Patokoski, J., Hellen, H., Hakola, H., Mogensen, D., Boy, M., Rinne, J., and Kulmala, M.: OH reactivity measurements within a boreal forest: Evidence for unknown reactive emissions, Environ. Sci. Technol., 44, 6614–6620, 2010.

Stavrakou, T., Peeters, J., and Müller, J.-F.: Improved global modelling of HOx recycling in isoprene oxidation: evaluation against the GABRIEL and INTEX-A aircraft campaign measurements, Atmos. Chem. Phys., 10, 9863–9878, doi:10.5194/acp-10-9863-2010, 2010.

Tan, D., Faloona, I., Simpas, J. B., Brune, W., Shepson, P. B., Couch, T. L., Sumner, A. L., Carroll, M. A., Thornberry, T., Apel, E., Riemer, D., and Stockwell, W.: HO_x budgets in a deciduous forest: Results from the prophet summer 1998 campaign, J. Geophys. Res.-Atmos., 106, 24407–24427, 2001.

Thornberry, T., Carroll, M. A., Keeler, G. J., Sillman, S., Bertman, S. B., Pippin, M. R., Ostling, K., Grossenbacher, J. W., Shepson, P. B., Cooper, O. R., Moody, J. L., and Stockwell, W. R.: Observations of reactive oxidized nitrogen and speciation of NO_y during the PROPHET summer 1998 intensive, J. Geophys. Res.-Atmos., 106, 24359–24386, 2001

Taraborrelli, D., Lawrence, M. G., Butler, T. M., Sander, R., and Lelieveld, J.: Mainz Isoprene Mechanism 2 (MIM2): an isoprene oxidation mechanism for regional and global atmospheric modelling, Atmos. Chem. Phys., 9, 2751–2777, doi:10.5194/acp-9-2751-2009, 2009.

Williams, J., Pöschl, U., Crutzen, P. J., Hansel, A., Holzinger, R., Warneke, C., Lindinger, W., and Lelieveld, J.: An atmospheric chemistry interpretation of mass scans obtained from a proton transfer mass spectrometer flown over the tropical rainforest of Surinam, J. Atmos. Chem., 38, 133–166, 2001.

Zhao, J., Zhang, R. Y., Fortner, E. C., and North, S. W.: Quantification of hydroxycarbonyls from OH-isoprene reactions, J. Am. Chem. Soc., 126, 2686–2687, 2004.